

Synthesis and Structural Characterization of Sm(II) and Yb(II) Complexes Containing Sterically Demanding, Chelating Secondary Phosphide Ligands

Keith Izod,* Paul O'Shaughnessy, Joanne M. Sheffield, William Clegg, and Stephen T. Liddle

Department of Chemistry, University of Newcastle upon Tyne, Newcastle upon Tyne, NE1 7RU, U.K.

Received March 14, 2000

Metathesis between $[(\text{Me}_3\text{Si})_2\text{CH}](\text{C}_6\text{H}_4\text{-2-OMe})\text{P}(\text{K})$ and $\text{SmI}_2(\text{THF})_2$ in THF yields $[(\text{Me}_3\text{Si})_2\text{CH}](\text{C}_6\text{H}_4\text{-2-OMe})\text{P}_2\text{Sm}(\text{DME})(\text{THF})$ (**1**), after recrystallization. A similar reaction between $[(\text{Me}_3\text{Si})_2\text{CH}](\text{C}_6\text{H}_3\text{-2-OMe-3-Me})\text{P}(\text{K})$ and $\text{SmI}_2(\text{THF})_2$ yields $[(\text{Me}_3\text{Si})_2\text{CH}](\text{C}_6\text{H}_3\text{-2-OMe-3-Me})\text{P}_2\text{Sm}(\text{DME})\cdot\text{Et}_2\text{O}$ (**2**), while reaction between $[(\text{Me}_3\text{Si})_2\text{CH}](\text{C}_6\text{H}_4\text{-2-CH}_2\text{NMe}_2)\text{P}(\text{K})$ and either $\text{SmI}_2(\text{THF})_2$ or YbI_2 yields the five-coordinate complex $[(\text{Me}_3\text{Si})_2\text{CH}](\text{C}_6\text{H}_4\text{-2-CH}_2\text{NMe}_2)\text{P}_2\text{Sm}(\text{THF})$ (**3**) or the solvent-free complex $[(\text{Me}_3\text{Si})_2\text{CH}](\text{C}_6\text{H}_4\text{-2-CH}_2\text{NMe}_2)\text{P}_2\text{Yb}$ (**4**), respectively. X-ray crystallography shows that complex **2** adopts a distorted cis octahedral geometry, while complex **1** adopts a distorted pentagonal bipyramidal geometry (**1**, triclinic, $P\bar{1}$, $a = 11.0625(9)$ Å, $b = 15.924(6)$ Å, $c = 17.2104(14)$ Å, $\alpha = 72.327(2)^\circ$, $\beta = 83.934(2)^\circ$, $\gamma = 79.556(2)^\circ$, $Z = 2$; **2**, monoclinic, $P2_1$, $a = 13.176(4)$ Å, $b = 13.080(4)$ Å, $c = 14.546(4)$ Å, $\beta = 95.363(6)^\circ$, $Z = 2$). Complex **3** crystallizes as monomers with a square pyramidal geometry at Sm and exhibits short contacts between Sm and the *ipso*-carbon atoms of the ligands (**3**, monoclinic, $C2/c$, $a = 14.9880(17)$ Å, $b = 13.0528(15)$ Å, $c = 24.330(3)$ Å, $\beta = 104.507(2)^\circ$, $Z = 4$). Whereas preliminary X-ray crystallographic data for **4** indicate a monomeric structure in the solid state, variable-temperature ^1H , $^{13}\text{C}\{^1\text{H}\}$, $^{31}\text{P}\{^1\text{H}\}$, and ^{171}Yb NMR spectroscopies suggest that **4** undergoes an unusual dynamic process in solution, which is ascribed to a monomer–dimer equilibrium in which exchange of the bridging and terminal phosphide groups may be frozen out at low temperature.

Introduction

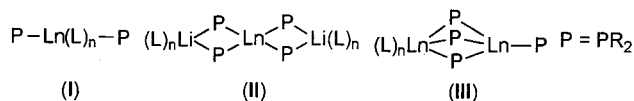
While the chemistry of the three lanthanide elements (Sm, Eu, and Yb) which may routinely be isolated in the +2 oxidation state has become relatively well established, the majority of reported complexes of these ions contain hard donor ligands such as halides, alkoxides, amides, or (substituted) cyclopentadienyl ligands.^{1–6} However, over the past decade there have been significant advances in the synthesis of lanthanide(II) complexes with alternative ligand systems,⁷ including ligands with donor atoms such as S, Se,^{8–11} C,^{12–15} Si, Ge, and Sn.^{16–18}

Perhaps some of the greatest progress in this area has been in the synthesis of Ln(II) complexes with P- and As-donor ligands.^{19–30} A number of samarium(II), europium(II), and ytterbium(II) diorganophosphides have now been synthesized and structurally characterized, including complexes with PPh_2 , $\text{P}(\text{mes})_2$ [$\text{mes} = 2,4,6\text{-Me}_3\text{-C}_6\text{H}_2$] and relatively bulky secondary phosphide ligands such as $\text{P}(\text{SiMe}_3)_2$.^{21–30} The structures adopted by these complexes are markedly affected by the presence of additional coligands such as THF or DME, although the exact nature of such solvates is often difficult to predict (THF = tetrahydrofuran, DME = 1,2-dimethoxyethane). Crystallographic studies have revealed three typical structural motifs

* To whom correspondence should be addressed. E-mail: k.j.izod@ncl.ac.uk.

- Anwander, R.; Herrmann, W. A. *Top. Curr. Chem.* **1996**, *179*, 1.
- Anwander, R. *Top. Curr. Chem.* **1996**, *179*, 33.
- Anwander, R. *Top. Curr. Chem.* **1996**, *179*, 149.
- Edelmann, F. T. *Angew. Chem., Int. Ed. Engl.* **1995**, *34*, 2466.
- Evans, W. J. *Polyhedron* **1987**, *6*, 803.
- van der Hende, J. R.; Hitchcock, P. B.; Lappert, M. F. *J. Chem. Soc., Dalton Trans.* **1995**, 2251. van der Hende, J. R.; Hitchcock, P. B.; Holmes, S. A.; Lappert, M. F. *J. Chem. Soc., Dalton Trans.* **1995**, 1435.
- Nief, F. *Coord. Chem. Rev.* **1998**, *178*, 13.
- Strzelecki, A. R.; Likar, C. L.; Helsel, B. A.; Utz, T.; Lin, M. C.; Bianconi, P. A. *Inorg. Chem.* **1994**, *33*, 5188.
- Nief, F.; Ricard, L. *Chem. Commun.* **1994**, 2723.
- Cetinkaya, B.; Hitchcock, P. B.; Lappert, M. F.; Smith, R. G. *Chem. Commun.* **1992**, 932.
- Carey, R. C.; Arnold, J. *Inorg. Chem.* **1994**, *33*, 1791.
- Eaborn, C.; Hitchcock, P. B.; Izod, K.; Smith, J. D. *J. Am. Chem. Soc.* **1994**, *116*, 12071.
- Eaborn, C.; Hitchcock, P. B.; Izod, K.; Lu, Z.-R.; Smith, J. D. *Organometallics* **1996**, *15*, 4783.
- Clegg, W.; Eaborn, C.; Izod, K.; O'Shaughnessy, P.; Smith, J. D. *Angew. Chem., Int. Ed. Engl.* **1997**, *36*, 2815.
- Hassinoff, L.; Takats, J.; Zhang, X. W.; Bond, A. H.; Rogers, R. D. *J. Am. Chem. Soc.* **1994**, *116*, 8833.
- Bochkarev, L. N.; Makarov, V. M.; Zakharov, L. N.; Fukin, G. K.; Yanovsky, A. I.; Struchkov, Y. T. *J. Organomet. Chem.* **1994**, *467*, C3.
- Cloke, F. G. N.; Dalby, C. I.; Hitchcock, P. B.; Karamallakis, H.; Lawless, G. A. *Chem. Commun.* **1991**, 779.
- Bochkarev, L. N.; Makarov, V. M.; Zakharov, L. N.; Fukin, G. K.; Yanovsky, A. I.; Struchkov, Y. T. *J. Organomet. Chem.* **1995**, *490*, C29.
- Nief, F.; Ricard, L. *J. Organomet. Chem.* **1994**, *464*, 149.
- Nief, F.; Ricard, L.; Mathey, F. *Polyhedron* **1993**, *12*, 19.
- Atlan, S.; Nief, F.; Ricard, L. *Bull. Chim. Soc. Fr.* **1995**, *132*, 649.
- Rabe, G. W.; Riede, J.; Schier, A. *Inorg. Chem.* **1996**, *35*, 2680.
- Rabe, G. W.; Yap, G. P. A.; Rheingold, A. L. *Inorg. Chem.* **1995**, *34*, 4521.
- Rabe, G. W.; Riede, J.; Schier, A. *Inorg. Chem.* **1996**, *35*, 40.
- Nief, F.; Ricard, L. *J. Organomet. Chem.* **1997**, *529*, 357.
- Rabe, G. W.; Riede, J.; Schier, A. *Organometallics* **1996**, *15*, 439.
- Rabe, G. W.; Guzei, I. A.; Rheingold, A. L. *Inorg. Chem.* **1997**, *36*, 4914.
- Rabe, G. W.; Yap, G. P. A.; Rheingold, A. L. *Inorg. Chem.* **1997**, *36*, 3212.
- Rabe, G. W.; Riede, J.; Schier, A. *Main Group Chem.* **1996**, *1*, 273.
- Rabe, G. W.; Yap, G. P. A.; Rheingold, A. L. *Inorg. Chim. Acta* **1998**, *267*, 309.

for these compounds: solvated monomers (**I**), e.g., $[\text{Yb}(\text{PPh}_2)_2(\text{THF})_4]^{23}$ ate complexes (**II**), e.g., $[\text{Sm}\{(\text{P}^t\text{Bu}_2)_2\text{Li}(\text{THF})_2\}]^{22,24}$ and unsymmetrical dimeric species with bridging phosphido ligands (**III**), e.g., $[\{(\text{Me}_3\text{Si})_2\text{P}\}\text{Sm}\{\mu\text{-P}(\text{SiMe}_3)_2\}_3\text{Sm}(\text{THF})_3\}^{26}$



The large size of the Ln(II) ions and their consequent requirement for high coordination numbers has had the effect that, until now, there has been no report of an alkali-metal-free, homoleptic lanthanide(II) phosphide complex.

As part of a continuing program of research into the effect of sterically demanding, chelating ligands on the structures and reactions of their metal complexes, we have developed a range of potentially chelating diorganophosphido ligands and sought to investigate their complexes with the lanthanides.^{31,32} We are particularly interested in the effect of steric hindrance, chelate ring size, and donor group on metal coordination numbers and reactivities. In this regard, we have recently discovered that, while $[\{(\text{Me}_3\text{Si})_2\text{CH}\}(\text{C}_6\text{H}_3\text{-2-OMe-3Me})\text{P}\}_2\text{K}$ reacts with YbI_2 to give the expected diphosphido complex $[\{(\text{Me}_3\text{Si})_2\text{CH}\}(\text{C}_6\text{H}_3\text{-2-OMe-3-Me})\text{P}\}_2\text{Yb}(\text{THF})_2$ (**5**), $[\{(\text{Me}_3\text{Si})_2\text{CH}\}(\text{C}_6\text{H}_4\text{-2-OMe})\text{P}\}_2\text{K}$ reacts with YbI_2 to give a novel phosphido-alkoxide complex $[\{(\text{Me}_3\text{Si})_2\text{CH}\}(\text{C}_6\text{H}_4\text{-2-O})\text{P}\}_2\text{Yb}(\text{THF})_4 \cdot (\text{Et}_2\text{O})_4$ (**6**).³² We herein describe the synthesis and characterization of four new complexes of sterically demanding, donor-functionalized secondary phosphido ligands with samarium(II) and ytterbium(II) (**1–4**), including the first example of an alkali-metal-free, mononuclear lanthanide(II) diphosphido.

Experimental Section

General Procedures. All manipulations were carried out using standard Schlenk techniques under an atmosphere of dry nitrogen or argon. Ether, THF, DME, light petroleum (bp 40–60 °C), methylcyclohexane, and toluene were distilled from sodium, potassium, or sodium/potassium alloy under an atmosphere of dry nitrogen and stored over a potassium film (with the exception of THF and DME, which were stored over activated 4A molecular sieves). Deuterated toluene and THF were distilled from potassium, deoxygenated by three freeze-pump-thaw cycles, and stored over activated 4A molecular sieves. YbI_2 ,³³ $\text{SmI}_2(\text{THF})_2$,³⁴ $[\{(\text{Me}_3\text{Si})_2\text{CH}\}(\text{C}_6\text{H}_4\text{-2-OMe})\text{P}\}_2\text{K}$,³² $[\{(\text{Me}_3\text{Si})_2\text{CH}\}(\text{C}_6\text{H}_3\text{-2-OMe-3-Me})\text{P}\}_2\text{K}$,³² and $[\{(\text{Me}_3\text{Si})_2\text{CH}\}(\text{C}_6\text{H}_4\text{-2-CH}_2\text{-NMe}_2)\text{P}\}_2\text{K}$ ³¹ were prepared according to previously published procedures.

³¹P NMR spectra were recorded on a Bruker WM300 spectrometer operating at 121.5 MHz, and ¹⁷¹Yb NMR spectra were recorded on a JEOL Lambda500 spectrometer operating at 87.5 MHz. ¹H and ¹³C spectra were recorded on a Bruker AC200 spectrometer, operating at 200.1 and 50.3 MHz, respectively. ¹H and ¹³C chemical shifts are quoted in parts per million relative to tetramethylsilane, ³¹P chemical shifts are quoted relative to external 85% H₃PO₄, and ¹⁷¹Yb chemical shifts are quoted relative to external ($\eta^5\text{-C}_5\text{Me}_5$)₂Yb(THF)₂.³⁵ Elemental analyses were obtained by Elemental Microanalysis Ltd., Okehampton, U.K. Mass spectra were recorded on a Micromass Autospec M

spectrometer operating in EI mode at 70 eV. The facile solvent loss experienced by **1** and **2** is reflected in their NMR spectra and elemental analyses.

Preparation of $[\{(\text{Me}_3\text{Si})_2\text{CH}\}(\text{C}_6\text{H}_4\text{-2-OMe})\text{P}\}_2\text{Sm}(\text{DME})(\text{THF})$ (1**).** To a cold (−78 °C) solution of $\text{SmI}_2(\text{THF})_2$ (0.31 g, 0.57 mmol) in THF (10 mL) was added, dropwise, a solution of $[\{(\text{Me}_3\text{Si})_2\text{CH}\}(\text{C}_6\text{H}_4\text{-2-OMe})\text{P}\}_2\text{K}$ (0.35 g, 1.04 mmol) in THF (10 mL). This mixture was allowed to warm to room temperature and was stirred for 16 h. Solvent was removed in vacuo, and the residue was extracted into ether (30 mL) and filtered. Solvent was removed in vacuo, and the slightly sticky solid was recrystallized from cold (−30 °C) methylcyclohexane/ether (10 mL/1 mL) containing a few drops of DME as deep green needles of **1**. Yield: 0.34 g, 73%. Anal. Calcd for $\text{C}_{32}\text{H}_{62}\text{O}_4\text{P}_2\text{Si}_4\text{Sm}$ (molecular formula without THF): C, 46.00; H, 7.48. Found: C, 45.67; H, 7.22. ¹H NMR (d_8 -THF): δ −8.00 (2H, s, CHP), 2.25 (36H, s, br, SiMe₃), 3.30 (~5H, s, br, MeO (DME)), 3.32 (~3H, s, CH₂O (DME)), 4.75 (2H, t, J = 6.5 Hz, ArH), 5.65 (2H, s, ArH), 6.02 (2H, m, ArH), 7.68 (2H, m, ArH), 11.05 (6H, s, OMe).

Preparation of $[\{(\text{Me}_3\text{Si})_2\text{CH}\}(\text{C}_6\text{H}_3\text{-2-OMe-3-Me})\text{P}\}_2\text{Sm}(\text{DME}) \cdot \text{Et}_2\text{O}$ (2**).** To a solution of $\text{SmI}_2(\text{THF})_2$ (0.32 g, 0.58 mmol) in THF (15 mL) was added a solution of $[\{(\text{Me}_3\text{Si})_2\text{CH}\}(\text{C}_6\text{H}_3\text{-2-OMe-3-Me})\text{P}\}_2\text{K}$ (0.41 g, 1.17 mmol) in THF (15 mL). This mixture was stirred for 12 h, and then solvent was removed in vacuo. The residue was extracted into ether (20 mL) and filtered. Solvent was removed from the filtrate to give a slightly sticky green solid. Dark green crystals of **2** were obtained from cold (−30 °C) ether containing a few drops of DME. Yield: 0.38 g, 69%. Anal. Calcd for $\text{C}_{34}\text{H}_{66}\text{O}_4\text{P}_2\text{Si}_4\text{Sm}$ (molecular formula without Et₂O): C, 47.29; H, 7.70. Found: C, 46.88; H, 7.81. ¹H NMR (d_8 -THF): δ −3.21 (2H, s, br, CHP), 0.85 (36H, s, br, SiMe₃), 3.90 (6H, s, ArMe), 5.10 (2H, s, ArH), 5.21 (2H, s, ArH), 8.07 (6H, s, ArOMe), 8.21 (2H, d, ArH), 8.39 (~3H, s, br, OMe (DME)), 9.28 (~2H, s, br, CH₂O (DME)).

Preparation of $[\{(\text{Me}_3\text{Si})_2\text{CH}\}(\text{C}_6\text{H}_4\text{-2-CH}_2\text{NMe}_2)\text{P}\}_2\text{Sm}(\text{THF})$ (3**).** To a suspension of $\text{SmI}_2(\text{THF})_2$ (0.87 g, 1.586 mmol) in ether (10 mL) was added, dropwise, a solution of $[\{(\text{Me}_3\text{Si})_2\text{CH}\}(\text{C}_6\text{H}_4\text{-2-CH}_2\text{-NMe}_2)\text{P}\}_2\text{K}$ (1.15 g, 3.162 mmol) in THF (25 mL). This mixture was stirred at room temperature for 16 h. Solvent was removed in vacuo, and the residue was extracted into ether (30 mL) and filtered. Solvent was removed in vacuo from the filtrate, and the slightly sticky green solid was dissolved in methylcyclohexane/THF (10 mL/0.5 mL) and cooled to 5 °C for 12 h. Dark green rectangular blocks of **3** were isolated after this time. Yield: 1.12 g, 81%. Anal. Calcd for $\text{C}_{36}\text{H}_{70}\text{N}_2\text{O}_2\text{P}_2\text{Si}_4\text{Sm}$: C, 49.61; H, 8.09; N, 3.21. Found: C, 49.41; H, 8.07; N, 3.19. ¹H NMR (d_8 -toluene): δ −27.83 (2H), −11.78 (2H), −2.92 (2H), −2.23 (36H, SiMe₃), −1.52 (2H), 3.63 (4H, THF), 5.81 (12H, NMe₂), 9.19 (2H), 10.88 (2H), 12.00 (2H), 18.29 (4H, THF). MS (EI): m/z 800 [3, Sm(P–N)₂], 522 [3, Sm(P–N)₂ – C₆H₄CH₂NMe₂ – 2SiMe₃], 471 [12, Sm(P–N)], 196 [12, (P–N) – C₆H₄CH₂NMe₂], 73 [100, SiMe₃] [P–N = $\{(\text{Me}_3\text{Si})_2\text{CH}\}(\text{C}_6\text{H}_4\text{-2-CH}_2\text{NMe}_2)$].

Preparation of $[\{(\text{Me}_3\text{Si})_2\text{CH}\}(\text{C}_6\text{H}_4\text{-2-CH}_2\text{NMe}_2)\text{P}\}_2\text{Yb}$ (4**).** To a suspension of YbI_2 (0.50 g, 1.17 mmol) in cold (−10 °C) ether (30 mL) was added, dropwise, a solution of $[\{(\text{Me}_3\text{Si})_2\text{CH}\}(\text{C}_6\text{H}_4\text{-2-CH}_2\text{-NMe}_2)\text{P}\}_2\text{K}$ (0.85 g, 2.34 mmol) in THF (25 mL). This mixture was allowed to warm to room temperature and was stirred for 16 h. Solvent was removed in vacuo, and the oily residue was extracted into toluene (3 × 20 mL). This solution was concentrated to ~5 mL and was cooled to −30 °C overnight. The deep orange-red crystals of **4** were isolated, and residual solvent was removed in vacuo. Yield 0.83 g, 86%. Anal. Calcd for $\text{C}_{32}\text{H}_{62}\text{N}_2\text{P}_2\text{Si}_4\text{Yb}$: C, 46.75; H, 7.60; N, 3.41. Found: C, 46.89; H, 7.70; N, 3.45. ¹H NMR (d_8 -toluene, 378 K): δ 0.77 (36H, s, br, SiMe₃), 1.24 (2H, s, CHP) 2.19 (6H, s, br, NMe₂), 3.88 (4H, s, br, CH₂N), 6.99 (4H, s, br, ArH), 7.39 (2H, s, br, ArH), 7.85 (2H, s, br, ArH). ¹³C{¹H} NMR (d_8 -toluene, 298 K) δ 1.50 (br, SiMe₃), 2.82 (br, SiMe₃), 6.88 (d, J_{PC} = 67.2 Hz, CHP), 41.71, 45.14 (br, NMe₂), 65.47 (d, J_{PC} = 25.8 Hz, CH₂N), 118.00, 127.96, 129.36 (Ar), 130.59 (d, J_{PC} = 25.9 Hz, Ar), 132.13 (Ar), 158.53 (d, J_{PC} = 66.2 Hz, Ar). ³¹P-{¹H} NMR (d_8 -toluene, 297 K): δ −56.3 (J_{YbP} = 649.6 Hz). ¹⁷¹Yb NMR (d_8 -toluene, 297 K): δ 864 (t, J_{YbP} ~ 680 Hz). MS (EI): m/z 1291 [1.5, Yb₂(P–N)₃ – NMe], 1245 [0.3, Yb₂(P–N)₃ – SiMe₃], 973 [1.7, Yb₂(P–N)₃ – CH(SiMe₃)₂], 803 [85, Yb(P–N)₂ – Me].

(31) Clegg, W.; Doherty, S.; Izod, K.; Kagerer, H.; O'Shaughnessy, P.; Sheffield, J. M. *J. Chem. Soc., Dalton Trans.* **1999**, 1825.

(32) Clegg, W.; Izod, K.; Liddle, S. T.; O'Shaughnessy, P.; Sheffield, J. M. *Organometallics* **2000**, *19*, 2090.

(33) Tilley, T. D.; Boncella, J. M.; Berg, D. J.; Burns, C. J.; Andersen, R. A. *Inorg. Synth.* **1990**, *27*, 147.

(34) Watson, P. L.; Tulip, T. H.; Williams, I. *Organometallics* **1990**, *9*, 1999.

(35) Avent, A. G.; Edelman, M. A.; Lappert, M. F.; Lawless, G. A. *J. Am. Chem. Soc.* **1989**, *111*, 3423.

Table 1. Crystallographic Data for **1–3**

	1	2	3
empirical formula	C ₃₆ H ₇₀ O ₃ P ₂ -Si ₄ Sm	C ₃₈ H ₇₆ O ₃ P ₂ -Si ₄ Sm	C ₃₆ H ₇₀ N ₂ OP ₂ -Si ₄ Sm
fw	907.57	937.64	871.59
cryst syst	triclinic	monoclinic	monoclinic
space group	<i>P</i> 1	<i>P</i> 2 ₁	<i>C</i> 2/ <i>c</i>
<i>a</i> , Å	11.0625(9)	13.176(4)	14.9880(17)
<i>b</i> , Å	15.9246(12)	13.080(4)	13.0528(15)
<i>c</i> , Å	17.2104(14)	14.546(4)	24.330(3)
α , deg	72.327(2)		
β , deg	83.934(2)	95.363(6)	104.507(2)
γ , deg	79.556(2)		
<i>V</i> , Å ³	2836.8(4)	2495.9(13)	4608.1(9)
<i>Z</i>	2	2	4
<i>d</i> _{calcd} , g cm ⁻³	1.063	1.248	1.256
λ (Mo K α), Å	0.710 73	0.710 73	0.710 73
μ , mm ⁻¹	1.204	1.371	1.475
<i>T</i> , K	160	160	160
<i>R</i> , <i>R</i> _w ^a (<i>F</i> ² > 2 σ)	0.0648, 0.1696	0.1015, 0.2418	0.0386, 0.0854
<i>R</i> , <i>R</i> _w ^a (all data)	0.0915, 0.1890	0.1251, 0.2533	0.0426, 0.0868
<i>S</i> ^a	1.073	1.033	1.239

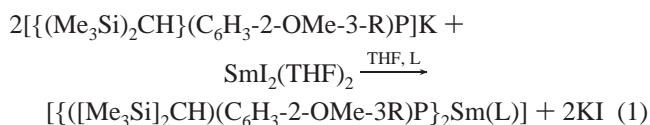
^a Conventional $R = \sum ||F_o| - |F_c|| / \sum |F_o|$; $R_w = [\sum w(F_o^2 - F_c^2)^2 / \sum w(F_o^2)^2]^{1/2}$; $S = [\sum w(F_o^2 - F_c^2)^2 / (\text{no. of data} - \text{no. of params})]^{1/2}$ for all data.

X-ray Data Collection and Structure Determination and Refinement for 1, 2, and 3. Crystal data are given in Table 1, and further details of the structure determinations are in the Supporting Information. Crystals were examined on a Bruker AXS CCD area-detector diffractometer. Intensities were integrated from more than a hemisphere of data recorded on 0.3° frames by ω rotation. Semiempirical absorption corrections were applied, based on symmetry-equivalent and repeated data.

The structures were solved variously by direct and heavy-atom methods and were refined by least-squares methods on all unique *F*² values, with anisotropic displacement parameters, and with constrained riding hydrogen atoms. All three structures display disorder. In **1** and **2** this involves alternative orientations of (Me₃Si)₂CH groups and is modeled with only moderate success, while disorder of the THF ligand in **3** over a 2-fold rotation axis is clearly resolved. Geometrical and displacement parameter restraints were applied to aid refinement in each case. The largest features in final difference syntheses were close to heavy atoms and disorder sites. Programs were standard Bruker AXS control and integration software and SHELXTL (Bruker AXS Inc., Madison, WI). Complete results can be found in the Supporting Information.

Results and Discussion

Synthesis and Characterization of Lanthanide Phosphides 1–4. Metathesis between the potassium salt [{(Me₃Si)₂CH}(C₆H₄-2-OMe)P]K or [{(Me₃Si)₂CH}(C₆H₃-2-OMe-3-Me)P]K and SmI₂(THF)₂ in ether solvents gives the novel lanthanide(II) phosphide complexes **1** or **2**, respectively, after recrystallization from cold methylcyclohexane/ether/DME or ether/DME mixtures (eq 1). These compounds are isolated in high yield after a simple workup, as deep green, air-sensitive crystals which are soluble in ether solvents but only slightly soluble in hydrocarbons.

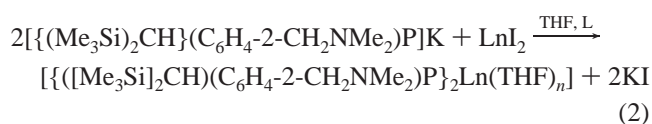


[**1**, R = H, L = (THF)(DME); **2**, R = Me, L = (DME)]

The facile formation of **1** contrasts markedly with reactions of the same potassium phosphides with YbI₂: while [{(Me₃Si)₂CH}(C₆H₃-2-OMe-3-Me)P]K reacts with YbI₂ to give the

expected diphosphide complex [{{(Me₃Si)₂CH}(C₆H₃-2-OMe-3-Me)P}₂Yb(THF)₂] (**5**), [{{(Me₃Si)₂CH}(C₆H₄-2-OMe)P]K reacts with YbI₂ under similar conditions to give the unprecedented alkoxy-phosphide complex [{{(Me₃Si)₂CH}(C₆H₄-2-O)P}₂Yb(THF)₄·(Et₂O)₄] (**6**) via a ligand cleavage reaction.³² No such ligand reactivity is observed in the reaction of [{{(Me₃Si)₂CH}(C₆H₄-2-OMe)P]K with SmI₂(THF)₂, suggesting, since redox chemistry is apparently not involved in the ligand cleavage reaction, that the reactivity observed with ytterbium is due largely to the increased Lewis acidity of the smaller Yb(II) ion.

The related samarium(II) and ytterbium(II) complexes **3** and **4** were synthesized in a manner analogous to the syntheses of **1** and **2** from [{{(Me₃Si)₂CH}(C₆H₄-2-CH₂NMe₂)P]K and either SmI₂(THF)₂ or YbI₂, respectively, in ether/THF solutions (eq 2). In contrast to **1** and **2** compounds **3** and **4** are soluble in nonpolar solvents such as toluene, light petroleum, or methylcyclohexane and may be recrystallized from cold solutions in these solvents.



[**3**, Ln = Sm, *n* = 1; **4**, Ln = Yb, *n* = 0]

The ¹H NMR spectra of the paramagnetic samarium(II) complexes **1**, **2**, and **3** are quite broad, with signals lying in the range -8 to +12 ppm for **1** and **2** and between -28 and +18 ppm for **3**; all are consistent with monomeric complexes having additional solvation by THF or DME. In the cases of **1** and **2** the coordinated solvent and solvent of crystallization are readily lost under vacuum; however, the coordinated THF in **3** is apparently tightly held and is not lost even after prolonged exposure to a vacuum, possibly reflecting the low coordination number of the Sm center in **3**. Assignment of the peaks in the ¹H NMR spectra of **1** and **2** was achieved with the aid of 2-D ¹H-¹H TOCSY and/or COSY experiments; however, these experiments gave no significant information about the signals in the ¹H NMR spectrum of **3**, and hence an unambiguous assignment of this spectrum was not possible. The typical ¹H chemical shift range for a Sm(II) complex is approximately -10 to +20 ppm;⁵ the unusually large ¹H chemical shift range observed for **3** may be a consequence of the close approach of the phenyl rings to the Sm(II) center, as observed in the solid state (see below), since the paramagnetic shift of a nucleus is a function of the internuclear separation between the paramagnetic center and the nucleus in question.³⁶

In contrast to **1–3**, multinuclear NMR spectroscopy and elemental analyses suggest that the diamagnetic compound **4** is isolated as the homoleptic, solvent-free complex [{{(Me₃Si)₂CH}(C₆H₄-2-CH₂NMe₂)P}₂Yb], despite being synthesized in the presence of the strongly coordinating ligand THF (a detailed discussion of the NMR spectra of **4** is presented below). This is somewhat surprising given the ready isolation of the related complex **5**,³² in which the tighter five-membered chelate rings of the phosphide ligands might be expected to increase steric congestion at the metal center, as a six-coordinate THF adduct. However, it appears that the greater flexibility of the chelate rings in complexes of the aminomethyl-substituted phosphide ligand and the greater steric demands of the CH₂-NMe₂ substituent result in lower coordination numbers; the Sm(II) complex of this ligand (**3**) is itself only five-coordinate, in

(36) Harris, R. K. *Nuclear Magnetic Resonance Spectroscopy*; Longman: Harlow, U.K., 1986.

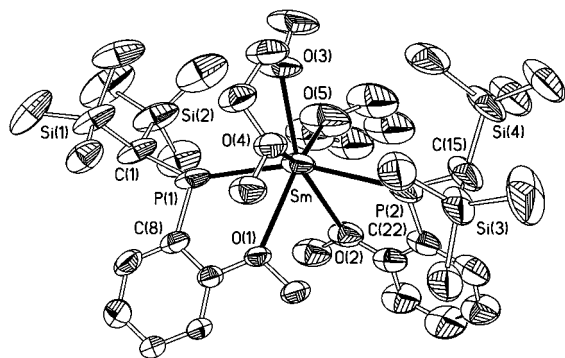


Figure 1. Molecular structure of **1** with 40% probability ellipsoids. H atoms and minor disorder components omitted for clarity. Selected bond lengths (Å) and angles (deg): Sm–P(1) 2.953(3), Sm–P(2) 2.955(3), Sm–O(1) 2.701(4), Sm–O(2) 2.685(5), Sm–O(3) 2.643(5), Sm–O(4) 2.607(5), Sm–O(5) 2.597(8), P(1)–C(1) 1.871(8), P(2)–C(15) 1.875(10), P(1)–C(8) 1.798(7), P(2)–C(22) 1.802(8), C(1)–Si(1) 1.875(6), C(1)–Si(2) 1.861(7), C(15)–Si(3) 1.988(10), C(15)–Si(4) 1.824(8), P(1)–Sm–P(2) 159.22(6), P(1)–Sm–O(1) 62.24(10), P(2)–Sm–O(2) 61.25(16), O(1)–Sm–O(2) 68.28(14), O(3)–Sm–O(4) 63.38(17), O(3)–Sm–O(5) 79.1(2), O(2)–Sm–O(5) 77.7(2), O(1)–Sm–O(4) 83.18(14), P(1)–Sm–O(5) 98.9(2), P(2)–Sm–O(5) 92.8(2), P(2)–Sm–O(1) 97.33(11), P(1)–Sm–O(2) 104.51(15), P(1)–Sm–O(3) 90.99(17), P(1)–Sm–O(4) 89.35(13), P(2)–Sm–O(3) 108.13(18), P(2)–Sm–O(4) 92.01(14).

comparison to the six- and seven-coordinate complexes **1** and **2**. Complex **4** represents the first example of a homoleptic, alkali-metal-free lanthanide(II) phosphide complex to be isolated; all previously reported lanthanide(II) phosphides crystallize as either ate complexes or solvated complexes containing additional donor ligands such as THF or *N*-methylimidazole.^{21–30}

Solid-State Structures of 1–4. Although all four lanthanide complexes **1–4** may be obtained in crystalline form, only **1**, **2**, and **3** gave crystals of suitable quality for a full X-ray crystallographic analysis. Both **1** and **2** crystallize from ether solutions containing a small amount of DME as dark black-green needles. The molecular structures of **1** and **2** are shown in Figures 1 and 2, respectively. Both complexes are monomeric in the solid state, with each phosphide ligand binding to the samarium centers through its phosphido P and ether O atoms to give five-membered chelate rings with P–Sm–O bite angles of 61.25(16)° and 62.24(10)° (**1**) and 62.5(4)° and 63.4(4)° (**2**). These bite angles are similar to that [60.9(2)°] reported for the related tridentate *O*-functionalized phosphide ligand in the binuclear complex [(Pr²N)₂La{μ-P(C₆H₄-2-OMe)₂}₂Li(THF)]·C₆H₅Me,³⁷ although the slightly smaller bite angle observed in this latter complex is a little surprising given the smaller ionic radius of La(III) compared to Sm(II) (1.10 vs 1.22 Å for a seven-coordinate species).³⁸ The coordination sphere of the Sm in **1** is completed by three oxygen atoms, two from a chelating DME ligand and one from a molecule of THF. The seven-coordinate Sm center adopts a distorted pentagonal bipyramidal geometry with the two phosphido groups in the apical positions [P(1)–Sm–P(2) 159.22(6)°], thus reducing steric interactions between the bulky CH(SiMe₃)₂ groups. In contrast, the samarium center in **2** is only six-coordinate. In addition to the two chelating phosphide ligands, the Sm center in **2** is coordinated by the two oxygen atoms of a chelating DME ligand, generating a highly distorted octahedral geometry. The phosphido groups are once again essentially mutually trans [P(1)–Sm–P(2) 127.09(18)°], thereby minimizing steric interactions between the bulky

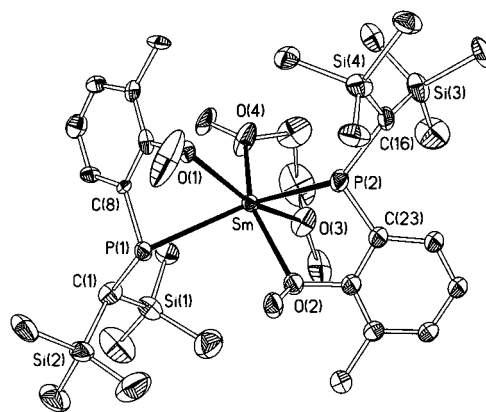


Figure 2. Molecular structure of **2** with 40% probability ellipsoids. H atoms and minor disorder components omitted for clarity. Selected bond lengths (Å) and angles (deg): Sm–P(1) 3.049(5), Sm–P(2) 2.988(6), Sm–O(1) 2.593(15), Sm–O(2) 2.556(13), Sm–O(3) 2.592(16), Sm–O(4) 2.48(2), P(1)–C(1) 1.89(2), P(2)–C(16) 1.906(19), P(1)–C(8) 1.796(18), P(2)–C(23) 1.80(2), C(1)–Si(1) 1.80(2), C(1)–Si(2) 1.96(3), C(16)–Si(3) 1.708(15), C(16)–Si(4) 1.875(14), P(1)–Sm–P(2) 127.09(18), P(1)–Sm–O(1) 62.5(4), P(2)–Sm–O(2) 63.4(4), O(1)–Sm–O(2) 111.7(5), O(3)–Sm–O(4) 66.4(7), O(1)–Sm–O(4) 93.8(5), P(2)–Sm–O(1) 86.3(4), P(1)–Sm–O(2) 88.5(3), P(1)–Sm–O(3) 125.3(4), P(1)–Sm–O(4) 111.5(5), P(2)–Sm–O(3) 98.8(4), P(2)–Sm–O(4) 112.2(6).

silyl substituents; the chelating DME ligand forces the oxygens of the two phosphide ligands to be mutually cis, contrasting with the all-trans geometry adopted by the related Yb(II) complex **5**.³²

The Sm–P distances of 2.953(3) and 2.955(3) Å in **1** are somewhat shorter than the same distances in **2** (2.988(6) and 3.049(5) Å), despite the higher coordination number in the former complex. These distances are at the lower end of the range of distances reported for Sm(II)–P bonds; indeed, the Sm(II)–P distances in **1** are the shortest such distances to be reported to date. For example, Sm(II)–P distances of 3.034(2) and 3.139(3) Å have been reported for the octahedral complexes [(mes)₂P}Sm(THF)₄]²⁵ and [(Ph₂P)₂Sm(*N*-MeIm)₄]²³ respectively (*N*-MeIm = *N*-methylimidazole), and distances of 3.019(3)–3.178(3) Å have been reported for the binuclear, phosphido-bridged complex [(THF)₃Sm{μ-P(SiMe₃)₂}₃Sm{P(SiMe₃)₂}].²⁶ The Sm(II)–P distances in the related η⁵-phospholyl complex [(2,3-dimethylphosphindolyl)₂Sm(THF)₂]¹⁹ and η¹-phospholyl complex [(dibenzophospholyl)₂Sm(THF)₄]²⁰ are 3.0775(1) and 3.1908(6) Å, respectively. The Sm–O(Ar) distances of 2.593(15) and 2.556(13) Å in **2** are similar to the Sm–O(DME) distances in this compound and are typical of Sm(II)–O(ether) distances.^{14,39–41} The Sm–O(Ar) distances of 2.701(4) and 2.685(5) Å in **1** are somewhat longer, possibly due to the increased steric congestion and higher coordination number of the metal center in this compound. Although the phosphide ligands in **2** are more sterically hindered than those in **1** due to the extra 3-Me group, it is found that the two P atoms in **1** are essentially planar (sum of angles at P(1) and P(2), 360.0° and 359.8°, respectively), while those in **2** are distinctly pyramidal (sum of angles at P(1) and P(2), 310.9° and 337.9°, respectively).

Complex **3** is chiral at the Sm center and crystallizes as a racemic mixture of enantiomeric pairs of five-coordinate

(37) Aspinall, H. C.; Moore, S. R.; Smith, A. K. *J. Chem. Soc., Dalton Trans.* **1993**, 993.

(38) Shannon, R. D. *Acta Crystallogr., Sect. A* **1976**, A32, 751.

(39) Evans, W. J.; Drummond, D. K.; Zhang, H.; Atwood, J. L. *Inorg. Chem.* **1988**, 27, 575.

(40) Evans, W. J.; Gummshheimer, T. S.; Ziller, J. W. *J. Am. Chem. Soc.* **1995**, 117, 8999.

(41) Minhas, R. K.; Ma, Y.; Song, J.-I.; Gambarotta, S. *Inorg. Chem.* **1996**, 35, 1866.

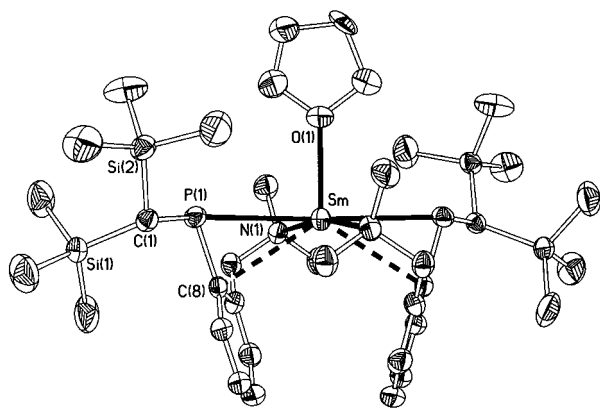


Figure 3. Molecular structure of **3** with 40% probability ellipsoids. H atoms and one THF disorder component omitted for clarity. Selected bond lengths (Å) and angles (deg): Sm–P(1) 3.0873(8), Sm–N(1) 2.682(3), Sm···C(8) 3.030(3), Sm–O(1) 2.535(3), P(1)–C(1) 1.892(3), P(1)–C(8) 1.831(3), C(1)–Si(1) 1.882(3), C(1)–Si(2) 1.874(3), P(1)–Sm–N(1) 75.01(6), P(1)–Sm–N(1′) 105.22(6), P(1)–Sm–O(1) 88.943(15), O(1)–Sm–N(1) 96.05(6), Sm–P(1)–C(8) 70.89(9), C(1)–P(1)–C(8) 103.83(13).

monomers with a distorted square pyramidal geometry about the samarium. The molecular structure of **3** is shown in Figure 3. Each phosphide ligand binds the Sm center through its P and N centers to give heavily puckered six-membered chelate rings. A molecule of THF completes the coordination sphere of Sm and lies at the apex of the square pyramid. The bite angle of the phosphide ligands of 75.01(6)° compares with bite angles for the same ligand of 81.40(4)° and 75.53(3)° in $[\{(Me_3Si)_2CH\}(C_6H_4-2-CH_2NMe_2)P]Na(tmeda)$ and $[\{(Me_3Si)_2CH\}(C_6H_4-2-CH_2NMe_2)P]K(pmdeta)$, respectively [tmeda = *N,N,N',N'*-tetramethylethylenediamine; pmdeta = *N,N,N',N',N''*-pentamethyldiethylenetriamine].³¹

The Sm–P distance of 3.0873(8) Å is slightly longer than the same distances in **1** and **2**, but lies well within the range of previously reported Sm(II)–P distances (see above). The Sm–N distance of 2.682(3) Å is similar to the Sm–N(*N*-MeIm) distances reported for the complexes *trans*-[Sm(C₁₂H₈N)₂(*N*-MeIm)₄] (2.685(14) Å)⁴² and [Sm(PPh₂)₂(*N*-MeIm)₄] (2.633(7) and 2.609(7) Å).²³ The P–Sm–P and N–Sm–N angles within the base of the square pyramid are 177.89(3)° and 167.89(12)°, respectively. As observed in **2** the phosphide ligands in **3** are distinctly pyramidal at the phosphorus atom (sum of angles at P, 305.82°).

One of the more notable features of the structure of **3** is the short contacts between the metal center and the aromatic rings of the ligands; in contrast to **1** and **2**, the formally five-coordinate Sm atom in **3** has short contacts with the *ipso*-carbons of the two phosphide ligands. The Sm–C(8) distance of 3.030(3) Å is a little longer than Sm(II)–C distances in complexes in which there is a strong Sm–C interaction such as the σ -alkyl complex [Sm{C(SiMe₃)₂(SiMe₂OMe)}₂(THF)] [Sm–C = 2.787(5) and 2.845(5) Å]¹⁴ and Cp*₂Sm(THF)₂ [Sm–C = 2.81(1)–2.91(1) Å].⁵ However, this appears to be a genuine Sm–C interaction: the phenyl rings in **3** are tilted toward the Sm atom, on the opposite, open, side of the SmP₂N₂ plane to the THF molecule, such that the Sm–P–C(8) angle is 70.89(8)°. This compares with Sm–P–C_{*ipso*} angles of 108.9(3)° and 109.2(4)° for the planar P atoms in **1** and 80.8(6)° and 94.5(7)° for the pyramidal P atoms in **2** (in both of these complexes there are no significant Sm···C contacts). The dihedral angle between the planes of the

two phenyl rings in **3** is approximately 32.3°, and the “folding angle” between the P–C(8)–C(13)–C(14) and (best fit) P–Sm–N–C(14) planes is approximately 84°. Similar M···C_{*ipso*} interaction and ligand folding are observed in the sodium and potassium complexes of this ligand, $[\{(Me_3Si)_2CH\}(C_6H_4-2-CH_2NMe_2)P]Na(tmeda)$ and $[\{(Me_3Si)_2CH\}(C_6H_4-2-CH_2NMe_2)P]K(pmdeta)$, for which the folding angles are close to 90°.³¹ Although such M···C_{*ipso*} contacts are a common feature of complexes of the electropositive metals of groups 1 and 2,⁴³ there are very few examples of such an interaction in a lanthanide complex.^{44–46} In the complex $[\{Me_2Al(\mu-Me)_2\}_2-Nd(\mu_3-NPh)(\mu-Me)AlMe_2]$, the phenylimido ligand bridges between the Nd and Al centers but also has a short contact (2.723(6) Å) between Nd and the *ipso*-carbon.⁴⁵ According to Shannon the difference in ionic radii between Nd³⁺ and Sm²⁺ should be approximately 0.16 Å,³⁸ the difference between the Nd···C_{*ipso*} distance in this latter complex and the Sm···C_{*ipso*} distance in **3** is almost twice this (0.307 Å). The mixed oxidation state Yb(II)/Yb(III) complex [Ph₂Yb(THF)(μ -Ph)₃Yb(THF)₃] also exhibits Yb···C contacts to the carbons *ortho* to the bridging C atom which range from 2.55(5) Å for the shortest Yb(III)–C_{*ortho*} contact to 2.67(3) Å for the longest Yb(II)–C_{*ortho*} distance.⁴⁶ Once again, the difference in Sm···C_{*ipso*} and Yb(II)–C_{*ortho*} distances in **3** and [Ph₂Yb(THF)(μ -Ph)₃Yb(THF)₃] of approximately 0.36–0.39 Å is significantly longer than the difference in ionic radii of Yb(II) and Sm(II) (~0.14 Å) would indicate, suggesting that the Sm–C_{*ipso*} interaction observed in **3** is probably quite weak.³⁸ As described above, the close approach of the aromatic rings to the paramagnetic Sm(II) center in **3** may be responsible for the extremely wide chemical shift range observed in its ¹H NMR spectrum.

Although crystals of compound **4** were obtained, these gave only poor crystallographic data despite repeated attempts at recrystallization, data collection, and refinement.⁴⁷ However, while these data are not sufficiently precise to enable a detailed analysis of bond lengths and angles within the molecule, they do provide an unambiguous picture of its connectivity (Figure 4). The Yb center is coordinated by the N and P atoms of two chelating phosphide ligands in a distorted tetrahedral geometry. No additional donor ligands are present, although the crystal structure contains one molecule of toluene per molecule of complex. This solvent is rapidly lost under vacuum and is not observed in the NMR spectra of **4** nor in its elemental analyses. As was observed in **3**, there are additional short contacts between the Yb center and the *ipso*-carbons of the two ligands, and once again, the phenyl rings lie on one side of the complex.

Solution-State Structure and Dynamic Behavior of **4**.

Although complex **4** could not be satisfactorily characterized by X-ray crystallography, its diamagnetic nature allowed a thorough investigation of the structure and dynamic behavior of this compound in solution by multielement NMR spectroscopy.

(43) For a recent review see: Smith, J. D. *Adv. Organomet. Chem.* **1999**, *43*, 267.

(44) A search of the Cambridge Crystallographic Database revealed only two examples of a lanthanide–*ipso*-carbon interaction (refs 45 and 46). Allen, F. H.; Kennard, O. *Chem. Des. Autom. News* **1993**, *8*, 31.

(45) Evans, W. J.; Ansari, M. A.; Ziller, J. W.; Khan, S. I. *Inorg. Chem.* **1996**, *35*, 5435.

(46) Bochkarev, M. N.; Khramenkov, V. V.; Rad'kov, Y. F.; Zakharov, L. N.; Struchkov, Y. T. *J. Organomet. Chem.* **1992**, *429*, 27.

(47) Crystals of **4** were monoclinic, space group *P2₁/n*, *a* = 19.424(4) Å, *b* = 11.415(2) Å, *c* = 22.150(5) Å, β = 107.241(3)°, *V* = 4690 Å³, *Z* = 4. They were of poor quality, giving marginal diffraction data, and the structure could not be satisfactorily refined, with *R* above 0.17, badly shaped displacement ellipsoids, and high residual electron density, indicating probable serious disorder problems that could not be resolved.

(42) Evans, W. J.; Rabe, G. W.; Ziller, J. W. *Organometallics* **1994**, *13*, 1641.

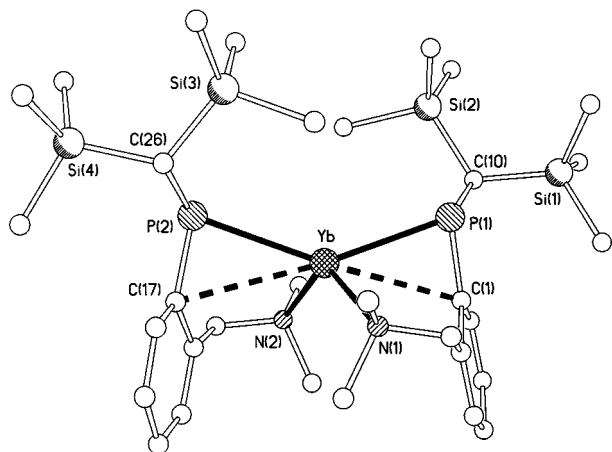
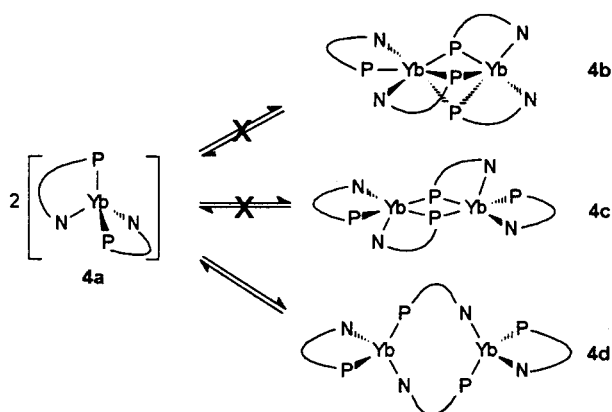


Figure 4. Molecular structure of **4**, as indicated qualitatively by X-ray crystallography.

Scheme 1



copy. At room temperature and below the ^1H NMR spectra of **4** are extremely broad and rather complicated, with many overlapping signals. As the temperature is raised the signals sharpen and simplify considerably until, at 105 °C, they are consistent with the presence of a monomeric, solvent-free, four-coordinate Yb(II) species containing equivalent phosphide ligands (**4a**; Scheme 1); i.e., the spectrum is consistent with the preliminary solid-state structure determined crystallographically. Although the complex is diastereomeric, only one set of ligand resonances is observed in the high-temperature ^1H NMR spectrum and only one signal is observed for the diastereotopic C(SiMe₃)₂, NMe₂, and CH₂N protons. This is most likely due to rapid, reversible P–Yb cleavage at this temperature, causing symmetrization of the P environment on the NMR time scale. A similar effect has been noted for the lithium, sodium, and potassium complexes of this ligand.³¹

The room temperature $^{31}\text{P}\{^1\text{H}\}$ NMR spectrum of **4** is also rather broad and consists of a single resonance at –56.3 ppm which exhibits satellites due to coupling to ^{171}Yb ($I = 1/2$, natural abundance 14%; $J_{\text{YbP}} = 650$ Hz). The presence and intensity of these satellites (each satellite comprises 7% of the overall intensity of the signal) are also consistent with structure **4a**. This signal also sharpens considerably at higher temperatures. However, as the temperature is reduced below ambient the intensity of this signal (A in Figure 5) decreases as a new, broad peak (B) begins to appear at –62.1 ppm. Below –40 °C this new signal splits into two signals of equal intensity at –61.2 (C) and –67.2 (D) ppm. These signals sharpen and increase in intensity as the temperature is lowered further, while peak A

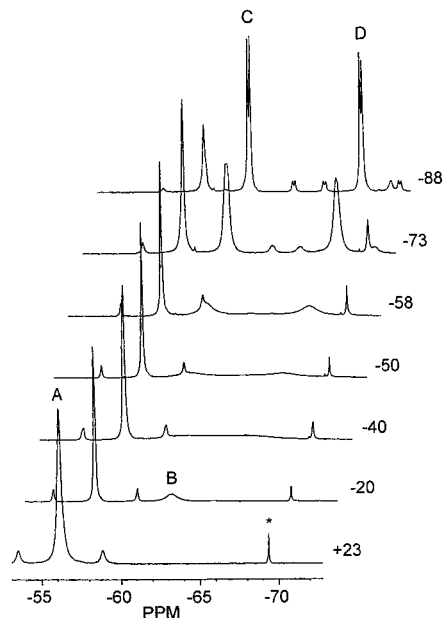


Figure 5. $^{31}\text{P}\{^1\text{H}\}$ NMR spectra of **4** between –88 and +23 °C. The asterisk indicates free secondary phosphine due to partial hydrolysis.

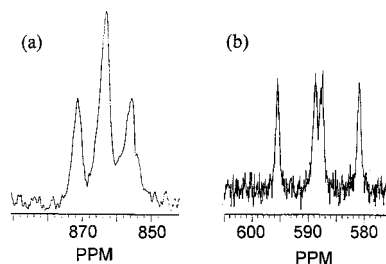


Figure 6. $^{171}\text{Yb}\{^1\text{H}\}$ NMR spectra of **4** at (a) 25 °C and (b) –75 °C.

continues to decrease in intensity and becomes sharper. Satellites due to coupling to ^{171}Yb become visible on both peaks C and D below –70 °C ($J_{\text{YbP}} = 577$ and 688 Hz, respectively; the high-field satellite of peak A is obscured by the main peak of signal C, and the low-field satellite of peak C is obscured by the main peak of signal A), clearly demonstrating that these signals are due to P atoms directly bonded to ytterbium. At –88 °C (the lowest temperature we were able to attain) signals C and D and their associated satellites are further resolved as doublets with $J_{\text{PP}} = 19.0$ Hz. At this temperature signals A, C, and D are in the approximate ratio 2:5:5.

These spectra are consistent with compound **4** undergoing a dynamic process in toluene solution that we ascribe to a monomer–dimer equilibrium in which the dimeric form predominates at low temperatures. As the temperature is reduced below ambient the concentration of monomer (peak A) decreases, while the concentration of dimer (peak B) increases. Below –50 °C signals due to the bridging and terminal phosphide ligands of the dimer are resolved (peaks C and D), and at the lowest available temperature these are clearly part of a simple XY spin system, with additional satellites due to coupling to ytterbium. At higher temperatures the bridging and terminal phosphide ligands in the dimer undergo rapid exchange, for which $\Delta G^\ddagger = 40.9$ kJ mol^{–1} at the coalescence temperature (–38 °C).

The ^{171}Yb NMR spectrum of **4** at room temperature consists of a 1:2:1 triplet ($J_{\text{YbP}} \approx 680$ Hz) at 864 ppm (Figure 6), again consistent with structure **4a**, in which one Yb center is coupled to two equivalent ^{31}P nuclei. At –75 °C the ^{171}Yb spectrum

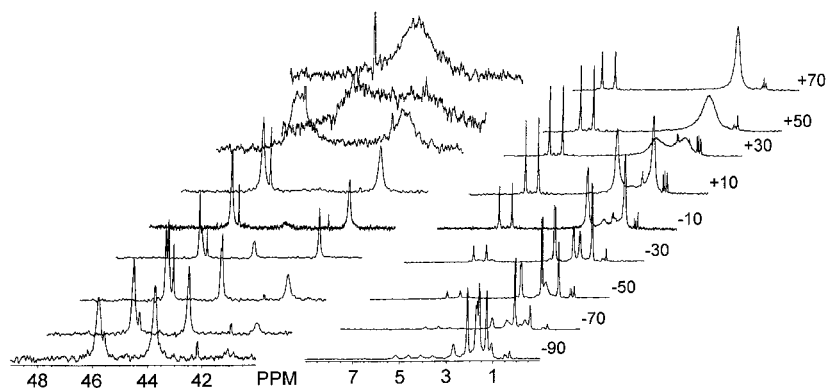


Figure 7. $^{13}\text{C}\{^1\text{H}\}$ NMR spectra of the NMe_2 and SiMe_3 regions of **4** between -90 and $+70$ °C.

consists of a doublet of doublets centered on 588 ppm ($J_{\text{YbP}} = 578$ and 688 Hz).

The possible structure of the dimeric form of **4** is of particular interest. The only previously reported example of a dimeric lanthanide(II) phosphide complex, $[\{(\text{Me}_3\text{Si})_2\text{P}\}\text{Sm}\{\mu\text{-P}(\text{SiMe}_3)_2\}_3\text{Sm}(\text{THF})_3]$, has three phosphide ligands bridging the two metal centers through their P atoms in a μ_2 -fashion.²⁶ The ^{31}P and ^{171}Yb NMR spectra described above clearly indicate that such a structure (**4b**; Scheme 1) is not adopted by complex **4**: if it were, the ^{171}Yb spectrum should consist of two distinct signals and the ^{31}P spectrum should exhibit two signals in a 3:1 ratio. Similarly, the alternative symmetrical structure **4c**, in which one of the two ligands on each Yb acts as both a chelating and a bridging ligand, would be expected to give rise to (a) two triplets of equal intensity in the ^{31}P NMR spectrum and (b) a complex doublet of doublets of doublets (as part of an $\text{ABB}'\text{X}$ spin system) in the ^{171}Yb spectrum. The sterically demanding $\text{CH}(\text{SiMe}_3)_2$ groups on each P center are likely to disfavor μ_2 -bridging via phosphorus in any case, since even a symmetrical dimer of type **4c** would require the coordination of three such centers to Yb in addition to two chelating nitrogen centers, giving a highly sterically crowded, five-coordinate metal center.

The observed low-temperature ^{31}P and ^{171}Yb spectra are consistent with a more unusual structural type, in which each Yb is coupled to only two, chemically inequivalent, P nuclei. This suggests a structure of type **4d** for the dimer in toluene solution, in which one aminophosphide acts solely as a chelating ligand to each Yb center and the two Yb atoms are bridged in a head-to-tail fashion by a pair of aminophosphide ligands, each binding to one Yb center through its P atom and to the other Yb center through its N atom. To our knowledge, such a structural type is without precedent in lanthanide(II) chemistry.

Variable-temperature $^{13}\text{C}\{^1\text{H}\}$ NMR spectra are also consistent with the dynamic behavior described above. While signals in the ^1H NMR spectrum are broad and exhibit significant overlap over the temperature range measured, signals in the ^{13}C NMR spectrum are more easily interpreted. Although **4** is diastereomeric in both the monomeric and proposed dimeric forms, at high temperatures the ^{13}C spectrum (Figure 7) exhibits only one resonance for the diastereotopic NMe_2 groups at 43.5 ppm and for the diastereotopic $\text{C}(\text{SiMe}_3)_2$ groups at 2.3 ppm, consistent with a monomeric complex in which reversible P–Yb and/or N–Yb cleavage leads to rapid interconversion both of the diastereotopic environments of the $\text{C}(\text{SiMe}_3)_2$ and NMe_2 groups and of the stereoisomeric forms of the monomer. Below 30 °C the SiMe_3 groups give rise to two peaks at 1.6 and 2.8 ppm. As the temperature is reduced below -10 °C a second pair of signals become evident at 1.8 and 2.2 ppm which we

assign to the diastereotopic/diastereomeric SiMe_3 groups in the dimer, averaged for the bridging and terminal ligands, which ^{31}P NMR spectra indicate are undergoing rapid exchange at this temperature. As the temperature is reduced still further these new signals increase in intensity at the expense of the monomer signals and split further until at -90 °C four signals of approximately equal intensity are observed at 1.4, 1.7, 1.8, and 2.2 ppm due to the bridging and terminal ligands, both of which have diastereotopic SiMe_3 groups (small signals remain for the SiMe_3 groups of the monomer at this temperature). The observed behavior of the NMe_2 resonances is somewhat simpler: The single resonance observed at high-temperature splits into two signals at 41.3 and 45.2 ppm below about 50 °C. As the temperature is reduced below -10 °C these are gradually replaced by two new signals at 42.8 and 44.9 ppm. These remain singlets down to -90 °C; a temperature low enough to observe the diastereotopicity of the NMe_2 groups could not be obtained. Similar behavior is exhibited by the Si_2CHP , benzylic, and aromatic carbon atoms; i.e., below -10 °C signals due to the monomer are gradually replaced by a new set of signals due to the dimer.

Mass spectral data indicate that **4** may also be dimeric in the gas phase: while the mass spectrum of **3** exhibits no peaks to higher mass than that of the molecular ion (m/z 800), the mass spectrum of **4** contains peaks of significant intensity at m/z 1291 and 973, which may be attributed to the fragments $\text{Yb}_2(\text{P-N})_3 - \text{NMe}$ and $\text{Yb}_2(\text{P-N})_3 - \text{CH}(\text{SiMe}_3)_2$, respectively [$\text{P-N} = \{(\text{Me}_3\text{Si})_2\text{CH}\}(\text{C}_6\text{H}_4\text{-2-CH}_2\text{NMe}_2)\text{P}$].

The isolation of a monomer in the solid state from a cold solution of **4** in toluene at first appears to contradict the observed predominance of a dimeric species at low temperatures. However, it is clear that, in toluene solution at least, the monomer is by far the most abundant species at the temperature at which crystals of **4** were grown (^{31}P NMR spectroscopy indicates a ratio of **4a**:**4d** of approximately 4:1 at -30 °C in this solvent), and so it is this monomeric species which crystallizes preferentially.

Conclusions

The samarium(II) and ytterbium(II) complexes of *O*- or *N*-functionalized, chelating secondary phosphide ligands are readily accessible by simple metathesis reactions between lanthanide(II) diiodides and the respective potassium phosphides. The structures adopted by these complexes are highly dependent upon the nature of the additional donor functionality of the ligand and on chelate ring size; the amino-functionalized ligand $\{(\text{Me}_3\text{Si})_2\text{CH}\}(\text{C}_6\text{H}_4\text{-2-CH}_2\text{NMe}_2)\text{P}$ has sufficient steric bulk to allow the isolation of complexes containing metals with very low coordination numbers (four and five for Yb and Sm,

respectively). Use of this ligand enables the synthesis of the first example of a homoleptic, solvent- and alkali-metal-free lanthanide phosphide complex, $[\{([Me_3Si]_2CH)(C_6H_4-2-CH_2-NMe_2)P\}_2Yb]$. The monomer–dimer equilibrium observed for this complex in solution suggests that the ligand provides just enough steric hindrance such that the complex lies on the cusp between steric saturation of the metal center and aggregation.

Acknowledgment. We thank Dr. M. N. S. Hill and Prof. W. McFarlane (Newcastle) for obtaining the NMR spectra. This

work was carried out with the support of the EPSRC and the Royal Society.

Supporting Information Available: X-ray crystallographic data (crystal data, structure solution and refinement, atomic coordinates, isotropic and anisotropic displacement parameters, and bond lengths and angles) for **1–3** and X-ray crystallographic files in CIF format. This material is available free of charge via the Internet at <http://pubs.acs.org>.

IC0002871